

CONSTRUCTION OF A TWO-MAGNET TYPE BROAD RANGE PARTICLE ANALYZER  
AND MEASUREMENT OF ION-OPTICAL PROPERTIES BY USE OF IT

N. Nakanishi, S. Motonaga, K. Matsuda,\* S. Takeda, M. Hemmi,  
T. Inoue, J. Fujita, H. Nakajima and Y. Awaya  
The Institute of Physical and Chemical Research  
Wako-shi, Saitama, Japan

Abstract

A magnetic analyzer used for nuclear reaction particles was constructed in association with the IPCR 160 cm cyclotron, by which the ion optical properties are determined.

The magnetic analyzer was designed to satisfy the following conditions, (i) momentum resolution of  $\Delta p/p < 2.5 \times 10^{-4}$ , (ii) luminosity of  $2.5 \times 10^3$  sr, (iii) large dispersion, (iv) small magnification of vertical image, (v) straight focal line and (vi) broadness of the momentum range of  $\pm 10\%$ . It is composed of two sectorial magnets which have a homogeneous magnetic field and curved pole boundaries. Such a complex configuration was chosen to meet the above conditions and ion optical properties. Two magnets have an air gap of 58 mm and their maximum magnetic rigidity and magnetic-motive force are  $1210 \text{ kG}\cdot\text{cm}$  along the standard trajectory and  $7.5 \times 10^4$  ampere turns, respectively. One of them is 32 tons and the other is 30 tons in total weight. The analyzer is rotated over an angular range from  $-15^\circ$  to  $140^\circ$  around the center of a 500 mm diam scattering chamber.

Some optical properties required are as follows: (i) deviation of the focal line from a straight line is less than 5 mm, (ii) momentum resolution and dispersion factor projected on the focal line are  $2.5 \times 10^{-4}$  and 6, respectively, on several points along the straight line, and (iii) solid angle is of about  $1.9 \times 10^3$  sr.

I. Introduction

Some kinds of a broad-range magnetic analyzer for nuclear reaction products have been developed and employed extensively as useful tools in nuclear spectroscopy. Many of these analyzers are composed of a single dipole magnet with homogeneous field.<sup>1,2,3</sup> However, recent development of the particle analyzer is directed to make use of a magnet of combined type in order to accomplish simultaneously such requirements as higher resolution, brighter luminosity, broader energy range and so on, or in order to improve more adequately only one or two certain optical properties. For example, there are a split-pole magnet, combined dipole magnet, quadrupole magnet followed by more than two dipole magnets and others.<sup>4,5,6</sup>

The present particle analyzer was designed to attain the following points: (1) remarkable dispersion factor, (2) high resolution, (3) high luminosity, (4) broadness of  $\pm 10\%$  of momentum

range, (5) small magnification, and (6) linearity of focal line.<sup>7</sup> In the single sectorial magnet the number of parameters is so small that we could not find a satisfactory solution. A particle analyzer composed of two homogeneous field magnets with curved pole boundaries was adopted, therefore. The spatial configuration of these magnets was determined by a graphical method, ray-tracing calculation as well as check of optical properties of the resultant magnet system.

The new particle analyzer was provided with a 500  $\phi$  scattering chamber of sliding membrane type and installed in the 160 cm IPCR cyclotron.

In Sect. 2 the field configuration and the ion optical properties of the magnetic analyzer are summarized. Description is given in Sects. 3 and 4 about constructive features and measured optical properties, respectively.

II. Brief Description of the Analyzer

Detailed explanation about the design of the present particle analyzer was already given in Ref. 7, so that a brief description only will be presented in this section.

Calculations were done considering that the fringing-field of a magnet was replaced by an equivalent sharp boundary and that these magnets were operated at the same magnetic field strength. In case of a system of two homogeneous magnets with curved pole boundaries, twelve parameters are available and all of them are adopted to search for optimum solutions. Then, some restrictions were introduced. The entrance and exit angles are kept at less than  $\pm 35^\circ$  because of not making the sharp boundary approximation worse, and the distance parameter between the two magnets is kept larger than the radius of the standard trajectory from mechanical consideration. Some criteria were also introduced to satisfy the conditions mentioned in the previous section. The change of dispersion on the radius of the trajectory is small. The horizontal and vertical focal points are not so far apart from each other. The deflection angle in the subsequent magnet is smaller than that in the preceding one because of lower cost.

Calculations for finding optimum parameter-families and their optical quantities were proceeded in four steps. In the first step sectorial magnet configurations and beam trajectories were constructed by the Cartan's graphical method and the first-order quantities of ion optics were calculated. After inspection, the higher-order optical properties were obtained by means of ray-tracing in the second and third steps. In the

\* deceased

final step, effects of all parameters available to optical properties were examined and then optimization of these parameters was carried out.

Figure 1 shows geometrical parameters of the particle analyzer and typical beam trajectories. The standard beam, which is an ideal beam of radius of 100.0 in the magnetic field corresponding to the acceptance angle of zero, goes from the point of object at a distance of 136.0 to the first magnet with an entrance angle of  $31.0^\circ$ . The beam is rotated by a deflection angle of  $78.5^\circ$  and goes out with an exit angle of  $17.0^\circ$ . The first magnet has entrance and exit boundaries of 241.0 and 370.0 in radius, respectively. The standard beam goes through the field-free region by a length of 180.0, and enters the second magnet with an angle of  $13.0^\circ$ . The boundaries of the second magnet are of 1800.0 in radius on the entrance side, and straight on the exit side. The standard beam is deflected by an angle of  $38.5^\circ$  and then goes out with an exit angle of  $-7.0^\circ$ , where the negative sign means that the pole edge provides vertical defocusing. The momentum range is analyzed simultaneously over  $\pm 10\%$  of the standard beam momentum. The highest and lowest momentum beams focus at a distance of 121.0 on the horizontal focal line. Beams with different momenta emerge almost parallel from the second magnet, and intersect with the horizontal focal line at an angle of  $35^\circ$ . The solid angle of 2.5 msr, dispersion factor of 6, full width of aberration of 0.2 and instrumental energy resolution of  $5 \times 10^{-4}$  are predicted. The horizontal and vertical magnifications are 1 and 2 at the first-order focal points, respectively. The curvature of the horizontal focal line is desirable to be small because of simple mechanism of detecting systems, and estimated to be less than 0.3.

### III. Practical Design of the Analyzer

The top view of the analyzer, some beam trajectories and peripheral devices are shown schematically in Fig. 2.

The standard beam is designed to be of the radius of 110.0 cm in the magnetic field, and therefore the maximum and minimum radii are taken to be 121.0 cm and 99.0 cm respectively. The magnets are operated at less than 11 kG in field strength because of avoiding iron saturation, and the magnetic rigidity is consequently limited to less than 1330 kG·cm. The magnets have an air gap of 58 mm and anti-scattering baffles are mounted at the exit side of both the magnets and at the entrance side of the second magnet. The truck, which holds the system of the particle analyzer, rotates from  $-15^\circ$  to  $140^\circ$  around the center of the scattering chamber. The system is connected through a sliding membrane with the chamber. These magnets have field-homogenizing air gaps of 5 mm between yoke and pole. The curved pole edge is shaped with removable pieces, and the pieces simulate for the designed curve stepwise. The magnet pole edge is displaced for the calculated boundary by 30 mm. As seen in Fig. 2, the NMR fluxmeter is used to measure and monitor the magnetic field. A vacuum pump system is applied through the connecting duct between two magnets. A solid state detector is mounted in front of the entrance of the first magnet and can be used as a beam monitor.

### IV. Conclusion and Discussion

More precise and more efficient particle analyzers have been getting to be required in the nuclear spectroscopy. There are two directions in

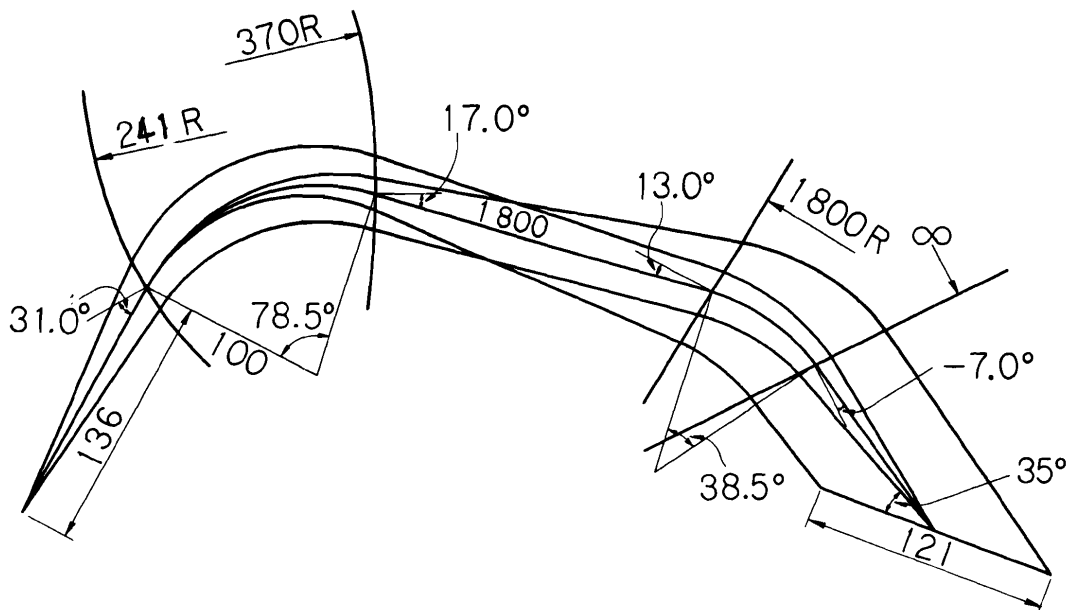


Fig. 1. The field configuration and parameters of the proposed particle analyzer.

its improvement. One of them is to design the analyzer so as to satisfy simultaneously and moderately the above-mentioned requirements and the other to have a certain excellent character at the sacrifice of other features. The proposed particle analyzer belongs to the former trially made.

Measurements of optical properties were carried out by two methods, a floating-wire method

and a method using particle beams. The former was employed in order to estimate roughly the position of a horizontal focal line, dispersion factors and incident angles to the focal line. According to this method, the horizontal focal distance was apt to be estimated somewhat longly. After that, alpha beams from  $^{210}\text{Po}$  nucleus, and proton and alpha beams from the cyclotron were used in order to calibrate the relation of the horizontal focal

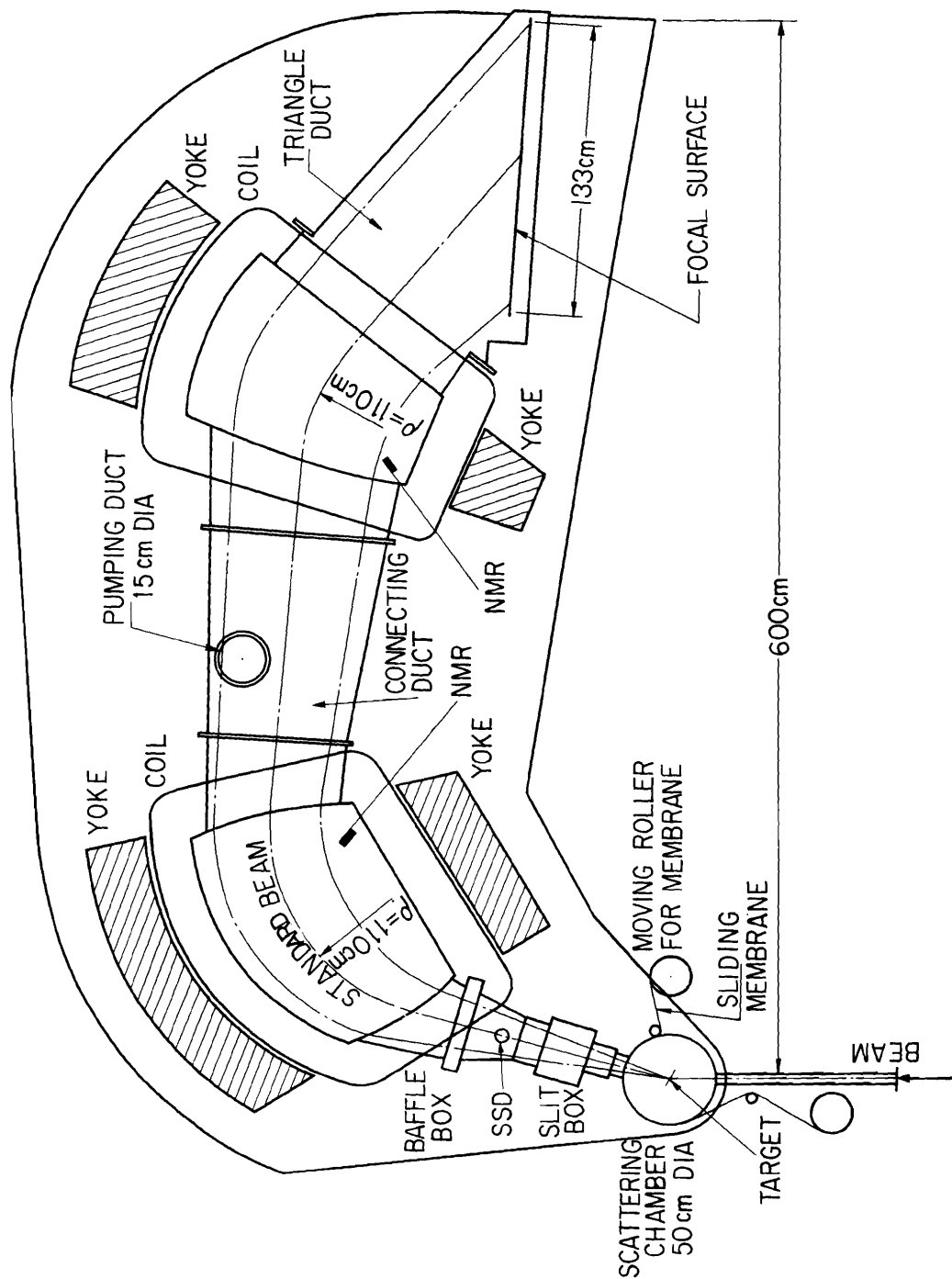


Fig. 2. The top view of the analyzing system and peripheral devices.

point to the beam radius, the solid angle and the dispersion factor. It was found through this method that beam trajectories were disturbed strongly by two vacuum ducts made of carbon steel. This fact was not found by the floating-wire method because of absence of these vacuum ducts. These ducts, that is, a connecting duct and a triangular duct, were replaced by those made of stainless steel. The horizontal focal points were again measured to confirm. In this case elastic scattering of 14 MeV proton by Au-target was measured and detected by a solid state detector. Beam aspects were examined at horizontal focal points in two directions by displacing the detector. Deviation along the focal line in the stainless steel duct is shown by a full line in Fig. 3, and that of carbon steel duct is also shown by a broken line. The slightly curved line becomes an optimum straight line by mounting nuclear plates.

Dispersion factors defined by  $\Delta s/\Delta p$  projected on the focal line were measured using proton beams. The result is shown in Fig. 4. Estimation of resolution was done in the same run as the above experiment. Proton beams from the cyclotron were analyzed in the energy accuracy of 0.1 % at 13.80 MeV and scattered elastically in the direction of  $14.75^\circ$  by Au of  $32.8 \mu\text{g}/\text{cm}^2$  thickness. Nuclear emulsion was used as a particle detector. The scattered beams were limited within an acceptance angle of  $\pm 0.76^\circ$ . Figure 5 shows an example

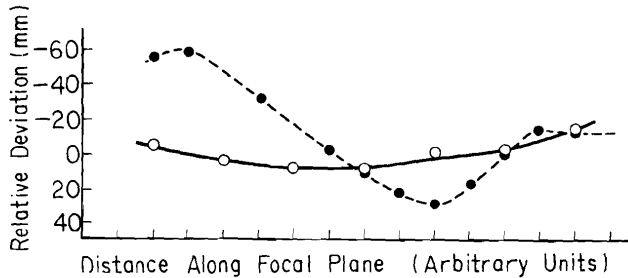


Fig. 3. Aspects of the horizontal focal line. A full and broken lines correspond to the case of stainless steel and carbon steel ducts, respectively.

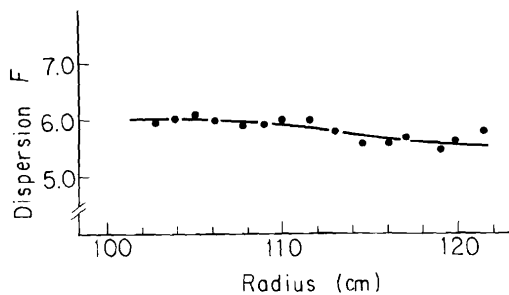


Fig. 4. Dispersion factor vs radius of curvature of beam.

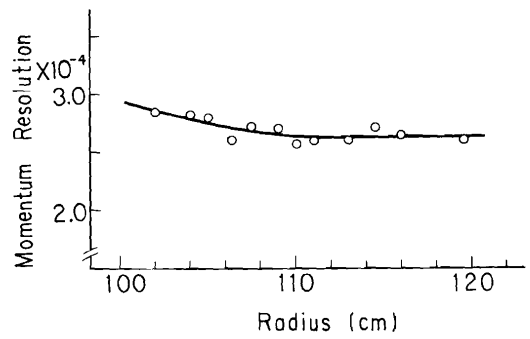


Fig. 5. A typical example of momentum resolution vs radius of curvature of beam.

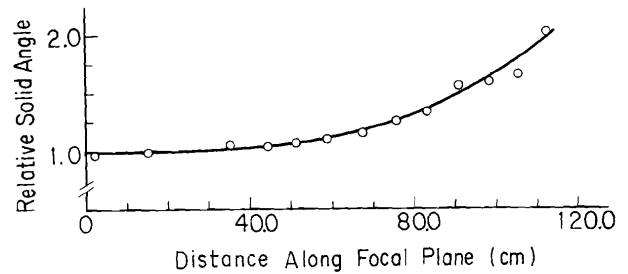


Fig. 6. Dependence of relative solid angle by horizontal focusing point.

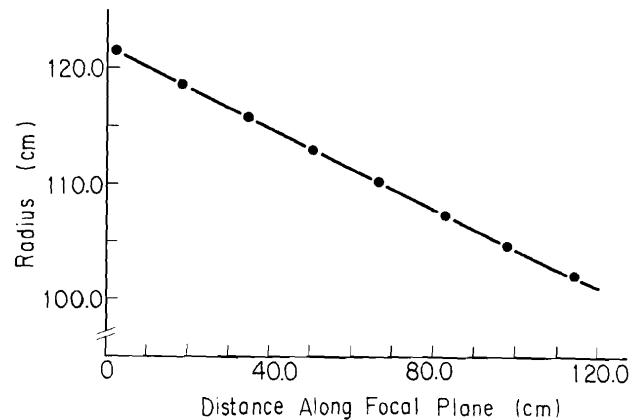


Fig. 7. Relation of the horizontal focusing point with the corresponding beam radius in the field.

of momentum resolution. Any correction is not applied because pure instrumental resolution is not so important for practical use. Solid angle was measured using 5.3 MeV and 40 MeV alpha beams and 14 MeV proton beam. Relative solid angle is shown in Fig. 6. For example, elastically scattered proton beams were detected by nuclear emulsion and these plates were scanned over a width of 8 mm. Absolute solid angle in this case is within the range from  $3.1 \times 10^{-4}$  sr to  $6.1 \times 10^{-4}$  sr when defining slits were set at an solid angle of  $8.2 \times 10^{-4}$ . Being translated into a designed

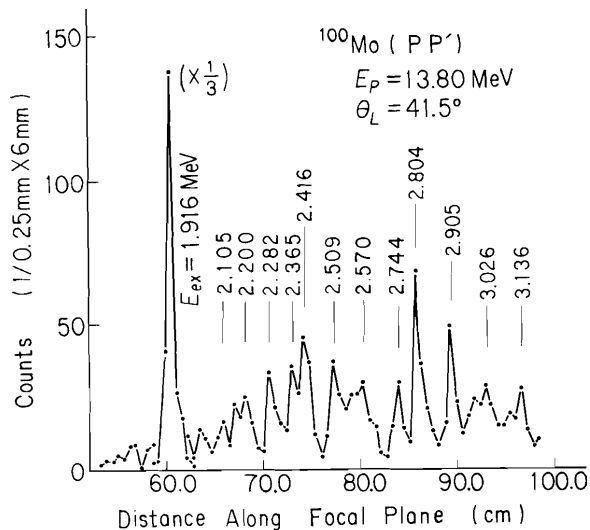


Fig. 8. Proton spectrum of a reaction  $^{100}\text{Mo}(p p')^{100}\text{Mo}$ . Excitation energies of some levels are shown, too. The target is of  $1.08 \text{ mg/cm}^2$  thickness.

condition the solid angle gets to  $1.9 \times 10^{-3}$  sr. This result agrees fairly well with values due to other beams.

Calibration for the relation between beam radius and focusing position was made using beams with four different momenta to examine the influence of field strength. These measurements were made in a magnetic field ranging from 2700 G to 3230 G for alpha beams from  $^{210}\text{Po}$ , from 4500 G to 5250 G for 14 MeV proton beams, from 4570 G to 5550 G for 16 MeV alpha beams and from 7440 G to 8850 G for 40 MeV alpha beams. The results are shown in Fig. 7. Slight systematic dependence by the field strength is observed, not being seen in this figure. The calibration was also done on the effect of hysteresis. Magnetic fields were set through two ways. One way was that exciting currents were directly set from zero to the necessary values and the other was that currents were set at the necessary values after being kept at twice of them for 15 min. Maximum difference of  $5 \times 10^{-4}$  was observed.

The proton energy spectrum of the reaction

$^{100}\text{Mo}(p p')^{100}\text{Mo}$  is shown in Fig. 8 in an excitation-energy range from 1.9 MeV to 3.2 MeV as an example. The proton beams of 13 MeV incident energy which were analyzed at energy resolution of less than 0.1 % were scattered by  $^{100}\text{Mo}$  nucleus at an angle of  $41.5^\circ$  and were detected by nuclear emulsion on the focal line. The target was a selfsupporting foil of  $1.08 \text{ mg/cm}^2$  thickness corresponding to the full energy loss of 19 keV. Nuclear plates were scanned in vertical width of 0.25 mm.

Predicted optical properties are roughly accomplished, but some unexpected facts are found in a stage of practical use. For example, there are difficulties of fixation of the relative position between two magnets and of the field reproducibility due to hysteresis. The former depends on the durability of the truck, rail and floor, and latter may be strongly influenced by fringing-field distribution through which beams proceed.

Development of a spark chamber and a solid state detector array as particle detectors mounted on the horizontal focal line is in progress.<sup>8</sup>

We are grateful to H. Kamitsubo for helpful discussions and are indebted the operating staff of the cyclotron laboratory for their assistance during these experiments.

#### References

1. C.P. Browne and W.W. Buechner, Rev. Sci. Instr. 27, 899 (1956).
2. J. Borggreen, B. Elbek and L.P. Nielsen, Nucl. Instr. and Meth. 24, 1 (1963).
3. A.E.S. Green, R.J. Berkley, C.E. Watson and C.F. Moore, Rev. Sci. Instr. 37, 415 (1966).
4. J.E. Spencer and H.A. Enge, Nucl. Instr. and Meth. 49, 181 (1967).
5. B. Klank, D.A. Lind and R.R. Johnson, Nucl. Instr. and Meth. 67, 61 (1969).
6. K. Yagi, Nucl. Instr. and Meth. 31, 173 (1964).
7. N. Nakanishi and K. Matsuda, Nucl. Instr. and Meth. 57, 245 (1967).
8. J. Fujita and S. Takeda, IPCR Cyclotron Progr. Rep. 5, 68 (1971), *ibid.* 4, 109 (1970).